AD-A158 009 THE DOWLING WALL PRESSURE-SPECTRUM ANALOGY APPLIED TO AN ISOTROPIC TWO-LA..(U) NAVAL UNDERWATER SYSTEMS CENTER NEW LONDON CT NEW LONDON LAB.. C A WAGNER 1/1

UNCLASSIFIED 14 NOV 84 NUSC-TR-7235 F/G 20/4 NL

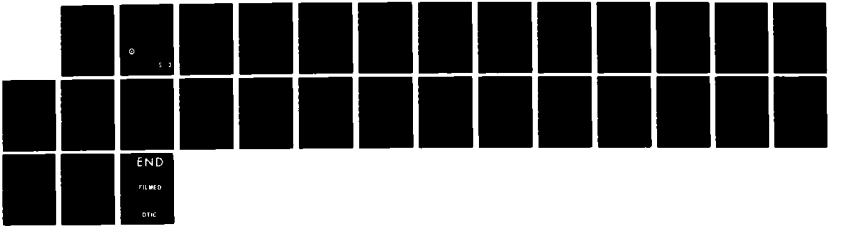

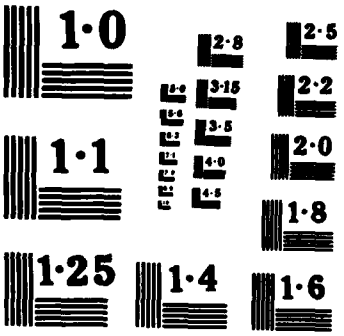

NATIONAL BUREAU OF STANDARDS
MICROCOPY RESOLUTION TEST CHART

AD-A158 009

NUSC Technical Report 7235
14 November 1984

The Dowling Wall Pressure-Spectrum Analogy Applied to an Isotropic Two-Layered Elastic Medium

Craig A. Wagner
Engineering and Technical Support Department

Naval Underwater Systems Center
Newport, Rhode Island / New London, Connecticut

DTIC FILE COPY

DTIC
ELECTE
JUL 2 9 1985
S D
G

Approved for public release; distribution unlimited.

Preface

This technical report was prepared under the IR/IED Program and NUSC Project No. A70200, Principal Investigator S. M. Rupinski (Code 3322). The sponsoring activity is Chief of Naval Material, Program Element 61152N, Navy Subproject No. ZR0000101, Program Manager Mr. Gary Morton (MAT-05).

The Technical Reviewer for this report was Dr. Roy C. Elswick (Code 10).

Reviewed and Approved: 14 November 1984

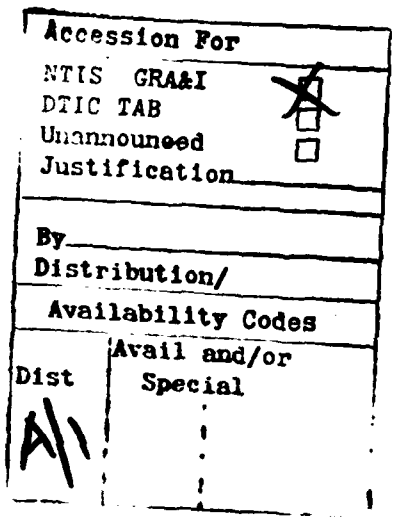

W. A. Von Winkle
Associate Technical Director
for Technology

The author of this report is located at the
New London Laboratory, Naval Underwater Systems Center,
New London, Connecticut 06320.

UNCLASSIFIED
SECURITY CLASSIFICATION OF THIS PAGE

REPORT DOCUMENTATION PAGE

1a. REPORT SECURITY CLASSIFICATION UNCLASSIFIED	1b. RESTRICTIVE MARKINGS
2a. SECURITY CLASSIFICATION AUTHORITY	3. DISTRIBUTION / AVAILABILITY OF REPORT Approved for public release; distribution unlimited.
2b. DECLASSIFICATION / DOWNGRADING SCHEDULE	
4. PERFORMING ORGANIZATION REPORT NUMBER(S) TR 7235	5. MONITORING ORGANIZATION REPORT NUMBER(S)
6a. NAME OF PERFORMING ORGANIZATION Naval Underwater Systems Center 6b. OFFICE SYMBOL (If applicable)	7a. NAME OF MONITORING ORGANIZATION
6c. ADDRESS (City, State, and ZIP Code) New London Laboratory New London, Connecticut 06320	7b. ADDRESS (City, State, and ZIP Code)
8a. NAME OF FUNDING / SPONSORING ORGANIZATION Naval Material Command 8b. OFFICE SYMBOL (If applicable) MAT-05	9. PROCUREMENT INSTRUMENT IDENTIFICATION NUMBER
8c. ADDRESS (City, State, and ZIP Code) Washington, DC 20360	10. SOURCE OF FUNDING NUMBERS PROGRAM ELEMENT NO. 61152N; PROJECT NO. ZR0000101; TASK NO.; WORK UNIT ACCESSION NO.

11. TITLE (Include Security Classification)
THE DOWLING WALL PRESSURE-SPECTRUM ANALOGY APPLIED TO AN ISOTROPIC TWO-LAYERED ELASTIC MEDIUM

12. PERSONAL AUTHOR(S)
Craig A. Wagner

13a. TYPE OF REPORT	13b. TIME COVERED FROM ____ TO ____	14. DATE OF REPORT (Year, Month, Day)	15. PAGE COUNT
		14 November 1984	

16. SUPPLEMENTARY NOTATION

17. COSATI CODES			18. SUBJECT TERMS (Continue on reverse if necessary and identify by block number)
FIELD	GROUP	SUB-GROUP	Turbulent Boundary Layer, Wall Pressure Spectrum

19. ABSTRACT (Continue on reverse if necessary and identify by block number)

The Dowling analogy applies Lighthill's equation to predict the surface pressure spectrum on a single elastic layer subjected to turbulent excitation. We have extended the analogy to obtain the low wavenumber surface pressure spectrum for an infinitely long two-layered isotropic elastic media. This low wavenumber model includes the effect of turbulent surface shear stresses on the wall pressure spectrum. The surface pressure spectrum is calculated on the surface of the elastic layer in contact with the turbulent fluid and for the interface between the two different elastic layers. Water is used for the turbulent fluid on one surface of the elastic media. Air at rest is used as the fluid media in contact with the opposite surface.

Pressure spectra are given first for the reduced case in which both layers are treated as steel of particular thicknesses at various frequencies. Then different elastic coatings are applied to the steel plates and the change in wall pressure spectra from that of the

20. DISTRIBUTION / AVAILABILITY OF ABSTRACT	21. ABSTRACT SECURITY CLASSIFICATION
☒ UNCLASSIFIED/UNLIMITED ☐ SAME AS RPT. ☐ DTIC USERS	UNCLASSIFIED
22a. NAME OF RESPONSIBLE INDIVIDUAL Craig A. Wagner	22b. TELEPHONE (Include Area Code) (203) 440-5339
	22c. OFFICE SYMBOL

DD FORM 1473, 84 MAR — 83 APR edition may be used until exhausted. All other editions are obsolete.

SECURITY CLASSIFICATION OF THIS PAGE
UNCLASSIFIED

cont'd

TABLE OF CONTENTS

THE DOWLING WALL PRESSURE-SPECTRUM ANALOGY APPLIED TO AN ISOTROPIC TWO-LAYERED ELASTIC MEDIUM

INTRODUCTION

The relative turbulent-boundary-layer wall pressure-spectrum characteristics on an elastic medium were predicted by Dowling through the solution of the Lighthill equation using Green's functions. The analogy is extended in this report to include a general two-layered isotropic elastic wall. The elastic wall is treated as a viscoelastic material through the use of complex shear and Young's moduli. The relative pressure-spectrum characteristics are given on the top surface of the layer of the elastic medium in contact with water and also at the surface between the two elastic layers. Air is assumed to be the fluid in contact with the back surface of the two-layered elastic wall. The effect of elastic-wall moduli and damping on the strength and location of surface-pressure singularities is shown to be rather significant.

BACKGROUND

The generation of noise produced by turbulent flows over elastic surfaces is the subject of much current research. Flow noise over aircraft bodies, jet noise, and noise generated by flow over underwater vehicles are but a few examples of problems in this area. In this report, we have extended the work of Dowling[1-3] to the analysis of the relative wall pressure spectrum on the surface of a two-layered elastic medium under a turbulent boundary layer in water. The other surface of the elastic medium is exposed to air at rest. Such an infinite configuration approximates that which occurs in a water tunnel with isotropic structural walls covered by an isotropic viscoelastic material. In the next section of this report, we derive the wall pressure spectrum due to turbulent flow by means of a Green-function analogy applied to Lighthill's equation describing the density field in the fluid. The following section incorporates the properties of the elastic layers into the expression for the surface pressure spectrum through the boundary conditions at the interface between the fluid and elastic medium. Our model also includes the effect of turbulent-boundary-layer shear stresses at the elastic surface. In the final section, we ~~examine~~ the structure of the pressure spectrum on a bare steel plate at 5 and 10 kHz. Then, we compare this to the pressure spectrum on the surface of two different viscoelastic layers applied to the steel plates. The results show that the propagation speeds of compressive, shear, and flexural waves in the elastic layers govern the location of singularities in the pressure spectra. It is also shown how damping can affect the strength of the singularities and the level of the local maxima.

Cont'd

Originator Supplied Keywords include:)

See DD 1473

SOLUTION TO LIGHTHILL EQUATION

The analogy derived for predicting the pressure spectrum on a single elastic layer through the solution to the Lighthill equation and elasticity equations is given in detail by Dowling.[3] In this section, we outline the general method of solving the Lighthill equation so we can show how the pressure spectrum couples to the two-layered elastic medium in the following section.

Our model is shown in figure 1.* For the flow speeds of interest in our underwater applications, the effect of the convected flow field is small and, therefore, does not appear as a parameter in the final analogy. Likewise, the boundary-layer thickness appears as a nondimensional parameter in the final equation for the pressure spectrum and not as an explicit variable. Also, we consider only surfaces whose mean displacement is linearly disturbed from rest position as this allows us to make some simplifications in the application of the Green-function solution at the surface and in linearizing the momentum equation. The assumptions and simplifications above allow us to proceed to solve the relative turbulent-boundary-layer wall-pressure problem.

The Lighthill equation describing the model in figure 1 is

$$\left(\frac{\partial^2}{\partial t^2} - c^2\nabla^2\right)(\rho - \rho_0) = \frac{\partial^2}{\partial y_i \partial y_j}\left\{\rho v_i v_j + \left[p - c^2(\rho - \rho_0)\right]\delta_{ij} - \sigma_{ij}\right\}_{i,j=1,2,3.} \tag{1}$$

Considering the source term on the right-hand side as a linear disturbance, we can apply the technique of Green functions to solve

$$\left(\frac{\partial^2}{\partial t^2} - c^2\nabla^2\right)G(\vec{y},\tau\,|\,\vec{x},t) = \delta(\vec{x} - \vec{y}, t - \tau) \ . \tag{2}$$

Superposition of this Green function with the source term will yield the density perturbations in the fluid and on the surface of the upper elastic layer.

The density perturbation given by taking the integral over the entire volume yields

$$(\rho - \rho_0)(\vec{x},t) = \int_V G\,\frac{\partial^2 T_{ij}}{\partial y_i \partial y_j}\,d^3\vec{y}d\tau \ . \tag{3}$$

Application of Green's theorem to equation (3) will give the volume and surface integrals,

*All figures have been placed together at the end of this report.

$$(\rho - \rho_0) = \int_V T_{ij} \frac{\partial^2 G}{\partial y_i \partial y_j} \, d^3\vec{y}d\tau$$

$$+ \int_S \left(-\rho_0 v_2 \frac{\partial G}{\partial \tau} - \sigma_{2\alpha} \frac{\partial G}{\partial y_\alpha} + p \frac{\partial G}{\partial y_2} \right)_{\alpha=1,3} dy_1 dy_3 d\tau \ . \qquad (4)$$

The quantities of particular interest to us are the Fourier transforms of the pressure spectrum taken in time and in the two horizontal directions. The Fourier transform taken on the surface integral, only (the overbars denote transformed variables), is shown by

$$(\rho - \rho_0)(\vec{x},t) = \int_V T_{ij} \frac{\partial^2 G}{\partial y_i \partial y_j} \, d\vec{y}d\tau + \frac{1}{(2\pi)^3} \int_S \Big\{ \bar{p}(0,\vec{k},\omega) \frac{\partial \bar{G}}{\partial y_2}(0,-\vec{k},-\omega)$$

$$+ i\left[\rho_0 \omega \bar{v}_2(0,\vec{k},\omega) + k_\alpha \bar{\sigma}_{2\alpha}(0,\vec{k},\omega)\right] \bar{G}(0,-\vec{k},-\omega) \Big\} d^2\vec{k}d\omega \ . \qquad (5)$$

If the Green function is chosen to make the surface integral vanish, we arrive at a boundary condition for this Green function, which is

$$\frac{\partial \bar{G}}{\partial y_2}(y_2,-\vec{k},-\omega) + iN(\vec{k},\omega)\bar{G}(y_2,-\vec{k},-\omega) = 0, \quad \text{at } y_2 = 0 \ , \qquad (6)$$

where $N(\vec{k},\omega) = \rho_0 \omega Z + k_\alpha Y_\alpha$. The functions Z and Y_α represent the generalized impedance functions, $Z(\vec{k},\omega) = \bar{v}_2(0,\vec{k},\omega)/\bar{p}(0,\vec{k},\omega)$ and $Y_\alpha = \bar{\sigma}_{2\alpha}(0,\vec{k},\omega)/\bar{p}(0,\vec{k},\omega)$. These impedance functions imply that the elastic deformation and fluid motion can be described in this linear fashion.

The Green function satisfying the boundary condition in equation (6) can be obtained directly and its derivative, $\partial^2/\partial y_i \partial y_j$, is given as

$$\frac{\partial^2 G}{\partial y_i \partial y_j}(\vec{y},\tau|\vec{x},t) = \frac{-1}{(2\pi)^3 ic^2} \int \frac{D_{ij}}{\gamma - N} e^{-i\omega(\tau-t) - ik_\alpha(y_\alpha - x_\alpha) - i\gamma y_2} d^2\vec{k}d\omega \ . \qquad (7)$$

The function D_{ij} is given as

$$D_{1,2} = D_{2,1} = K_1\gamma \qquad D_{1,1} = K_1^2 \qquad D_{2,2} = \gamma^2$$

$$D_{3,1} = D_{1,3} = K_1 K_3 \qquad D_{3,2} = D_{2,3} = K_3\gamma \qquad D_{3,3} = K_3^2 \ . \qquad (8)$$

The function γ is defined as $\left(\omega^2/c^2 - K_1^2 - K_3^2\right)^{1/2}$ and the appropriate roots to choose for γ when it is real or imaginary depend on the choice of branch cuts used in evaluating the Green function.

Inclusion of equation (7) into equation (5) will yield, after taking the transform,

$$\bar{p}(\vec{k},\omega) = - \frac{D_{ij}}{i(\gamma - N)} \int e^{-i\gamma y_2} \bar{T}_{ij}(y_2,\vec{k},\omega) dy_2 \ . \tag{9}$$

In equation (9), the pressure perturbation has been related to the density change through the expression $p = c^2(\rho - \rho_0)$. This relation implies a simple linear compressible (i.e., acoustic) relation of pressure fluctuations to density fluctuations.

To solve for the total-pressure spectrum, we take the cross correlation of both sides and obtain

$$\bar{P}(\vec{k},\omega) = - \frac{D_{ij}D^{+}_{k\ell}}{|\gamma - N|^2} \int e^{-i\gamma y_2 + i\gamma^{+} y_2'} \bar{T}_{ijk\ell}(y_2,y_2',\vec{k},\omega) dy_2 dy_2' \ . \tag{10}$$

The nature of $T_{ijk\ell}$, the Fourier transform of the turbulent source terms, is believed to be such that, in the low-wavenumber region of interest, the effect of the small displacements at the elastic surface and fluid compressibility do not appreciably alter the spectrum of the turbulent source terms. Therefore, one can nondimensionalize the pressure spectrum to obtain the final expression as

$$\bar{P}(\vec{k},\omega) = \frac{D_{ij}D^{+}_{k\ell}}{|\gamma - N|^2} \rho_0^2 U^3 h^5 Q_{ijk\ell} \ , \tag{11}$$

where h is the boundary-layer thickness and U is the free stream velocity above the boundary layer. The superscript plus denotes the complex conjugate and $Q_{ijk\ell}$ is the Fourier transform of the cross correlation of the turbulent source terms. To obtain the nature of the wall pressure spectrum, it remains only to relate the elastic properties to the impedance functions Z and Y_α.

ELASTIC IMPEDANCE FUNCTIONS

The elastic media described in this model are homogeneous, isotropic, and infinite in the horizontal directions. Therefore, we can simplify our model by considering one horizontal component only, since the other horizontal component can be obtained by a coordinate transformation applied to the reduced problem. We are essentially working in two-dimensional space.

For elastic waves in layered media, the velocities are given by Brekhovskikh.[4] Since $\vec{v} = i\omega\vec{u}$, the displacements will be given here as

$$\vec{u} = \nabla\phi + \nabla x\vec{\psi} \ , \tag{12}$$

where ϕ and $\vec{\psi}$ are functions of the material properties of the media;

$$\phi = A \sin\left(\frac{\omega^2}{c_i^2} - k_1^2\right)^{1/2} y + B \cos\left(\frac{\omega^2}{c_i^2} - k_1^2\right)^{1/2} y$$

and

$$\vec{\psi} = C \sin\left(\frac{\omega^2}{c_{si}^2} - k_1^2\right)^{1/2} y + D \cos\left(\frac{\omega^2}{c_{si}^2} - k_1^2\right)^{1/2} y \ ,$$

where c_i and c_{si} are the compressional and shear wave speeds in the i-th layer. A, B, C, and D are as yet undetermined coefficients that will be resolved through application of the boundary conditions. The wave speeds can be related to the elastic material constants,

$$c_i = \sqrt{\frac{\lambda_i + 2\mu_i}{\rho_i}}$$

$$c_{si} = \sqrt{\frac{\mu_i}{\rho_i}} \ , \tag{13}$$

where λ_i and μ_i are the Lame constants corresponding to the i-th layers and ρ_i is the mass density corresponding to the i-th layer.

With the two-dimensional situation, there are a total of four boundary conditions to be applied to each interface, continuity of normal stress, tangential stress, normal displacement, and tangential displacement. Denoting the upper fluid properties with no superscript and the upper medium, lower medium, and lower fluid with superscript prime, double prime, and triple prime, respectively, we arrive at 12 boundary conditions.

BOUNDARY CONDITIONS

At the Surface y = 0

Boundary conditions at the surface y = 0 are

$$-P = \sigma'_{22} = \lambda'\left(\frac{\partial^2\phi'}{\partial x^2} + \frac{\partial^2\phi'}{\partial y^2}\right) + 2\mu'\left(\frac{\partial^2\phi'}{\partial y^2} + \frac{\partial^2\psi'}{\partial x\partial y}\right)$$

$$= -\left[\lambda'\left(k_1^2 + \gamma'^2\right) + 2\mu'\gamma'^2\right]B' + 2i\mu' k_1 \gamma'_s C' \ ,$$

$$\sigma_{12} = \sigma'_{12} = \mu' 2\left(\frac{\partial^2\phi'}{\partial x \partial y} + \frac{\partial^2\psi'}{\partial x^2} - \frac{\partial^2\psi'}{\partial y^2}\right) = 2i\mu' k_1 \gamma' A' + \mu'\left(\gamma_s'^2 - k_1^2\right) D' ,$$

$$v_2 = v'_2 = iw\left(\frac{\partial\phi'}{\partial y} + \frac{\partial\psi'}{\partial x}\right) = i\omega\gamma' A' - \omega k_1 D' ,$$

and

$$v_1 = v'_1 = iw\left(\frac{\partial\phi'}{\partial x} - \frac{\partial\psi'}{\partial y}\right) = -\omega k_1 B' - i\omega\gamma'_s C' .$$

At the Surface $y = T_1$

Boundary conditions at the surface $y = T_1$ are

$$\sigma'_{22} = \sigma''_{22};\ -\left[\lambda'\left(k_1^2 + \gamma'^2\right) + 2\mu'\gamma'^2\right]\left(A' \sin \gamma' T_1 + B' \cos \gamma' T_1\right)$$

$$+ 2i\mu' k_1 \gamma'_s\left(C' \cos \gamma'_s T_1 - D' \sin \gamma'_s T_1\right)$$

$$= -\left[\lambda''\left(k_1^2 + \gamma''^2\right) + 2\mu''\gamma''^2\right]\left(A'' \sin \gamma'' T_1 + B'' \cos \gamma'' T_1\right)$$

$$+ 2i\mu'' k_1 \gamma''_s\left(C'' \cos \gamma''_s T_1 - D'' \sin \gamma''_s T_1\right) ,$$

$$\sigma'_{12} = \sigma''_{12};\ 2i\mu' k_1 \gamma'\left(A' \cos \gamma' T_1 - B' \sin \gamma' T_1\right)$$

$$+ \mu'\left(\gamma_s'^2 - k_1^2\right)\left(C' \sin \gamma'_s T_1 + D' \cos \gamma'_s T_1\right)$$

$$= 2i\mu'' k_1 \gamma''\left(A'' \cos \gamma'' T_1 - B'' \sin \gamma'' T_1\right)$$

$$+ \mu''\left(\gamma_s''^2 - k_1^2\right)\left(C'' \sin \gamma''_s T_1 + D'' \cos \gamma''_s T_1\right),$$

$$v'_2 = v''_2;\ \gamma'\left(A' \cos \gamma' T_1 - B' \sin \gamma' T_1\right) + ik_1\left(C' \sin \gamma'_s T_1 + D' \cos \gamma'_s T_1\right)$$

$$= \gamma''\left(A'' \cos \gamma'' T_1 - B'' \sin \gamma'' T_1\right) + ik_1\left(C'' \sin \gamma''_s T_1 + D'' \cos \gamma''_s T_1\right) ,$$

and

$$v'_1 = v''_1;\ ik_1\left(A' \sin \gamma' T_1 + B' \cos \gamma' T_1\right) - \gamma'_s\left(C' \cos \gamma_s T_1 + D' \sin \gamma'_s T_1\right)$$

$$= ik_1\left(A'' \sin \gamma'' T_1 + B'' \cos \gamma'' T_1\right) - \gamma''_s\left(C'' \cos \gamma''_s T_1 - D'' \sin \gamma''_s T_1\right) .$$

At the Surface $y = T_2$

Boundary conditions at the surface $y = T_2$ are

$$-p''' = \sigma''_{22} = -\left[\lambda''\left(k_1^2 + \gamma''^2\right) + 2\mu''\gamma''^2\right]\left(A'' \sin \gamma''T_2 + B'' \cos \gamma''T_2\right)$$

$$+ 2i\mu''k_1\gamma''_s\left(C'' \cos \gamma''_sT_2 - D'' \sin \gamma''_sT_2\right) ,$$

$$\sigma'''_{12} = \sigma''_{12} = 2i\mu''k_1\gamma''\left(A'' \cos \gamma''T_2 - B'' \sin \gamma''T_2\right)$$

$$+ \mu''\left(\gamma''^2_s - k_1^2\right)\left(C'' \sin \gamma''_sT_2 + D'' \cos \gamma''_sT_2\right) ,$$

$$v'''_2 = v''_2 = i\omega\gamma''\left(A'' \cos \gamma''T_2 - B'' \sin \gamma''T_2\right) - \omega k_1\left(C'' \sin \gamma''_sT_2 + D'' \cos \gamma''_sT_2\right) ,$$

and

$$v'''_1 = v''_1 = -\omega k_1\left(A'' \sin \gamma''T_2 - B'' \cos \gamma''T_2\right) - i\omega\gamma''_s\left(C'' \cos \gamma''_sT_2 - D'' \sin \gamma''_sT_2\right) .$$

FURTHER REDUCTION OF THE SYSTEM

Linearization of the momentum equation in the fluid results in two relationships that further reduce the system of equations. These relationships express tangential velocity, normal stress, and tangential stress as

$$v_1 = \frac{-\sigma_{12}}{\rho(i\omega\nu)^{1/2}} - \frac{k_1 p}{\rho\omega} . \tag{14}$$

On the lower surface, since the lower fluid is air at rest, the relationship between normal velocity and normal stress can be described as

$$v'''_2 = \frac{\gamma'''p'''}{\rho'''\omega} . \tag{15}$$

Using equations (14) and (15) in the boundary-condition equations and assembling the result in matrix form, we arrive at

$$\begin{bmatrix} a_{1,1} & a_{1,2} & a_{1,3} & \cdot & \cdot & \cdot & \cdot & a_{1,12} \\ a_{2,1} & a_{2,2} & \cdot & \cdot & \cdot & \cdot & \cdot & \cdot \\ a_{3,1} & \cdot & \cdot & \cdot & \cdot & \cdot & \cdot & \cdot \\ \cdot & \cdot & \cdot & \cdot & \cdot & \cdot & \cdot & \cdot \\ \cdot & \cdot & \cdot & \cdot & \cdot & \cdot & \cdot & \cdot \\ \cdot & \cdot & \cdot & \cdot & \cdot & \cdot & \cdot & \cdot \\ \cdot & \cdot & \cdot & \cdot & \cdot & \cdot & \cdot & \cdot \\ \cdot & \cdot & \cdot & \cdot & \cdot & \cdot & \cdot & \cdot \\ \cdot & \cdot & \cdot & \cdot & \cdot & \cdot & \cdot & \cdot \\ \cdot & \cdot & \cdot & \cdot & \cdot & \cdot & \cdot & \cdot \\ a_{12,1} & \cdot & \cdot & \cdot & \cdot & \cdot & \cdot & a_{12,12} \end{bmatrix} \cdot \begin{Bmatrix} A' \\ B' \\ C' \\ D' \\ A'' \\ B'' \\ C'' \\ D'' \\ \sigma_{12} \\ v_2 \\ \sigma'''_{12} \\ p''' \end{Bmatrix} = P \begin{Bmatrix} -1 \\ 0 \\ 0 \\ 0 \\ -k_1/\rho\omega \\ 0 \\ 0 \\ 0 \\ \cdot \\ \cdot \\ 0 \\ 0 \end{Bmatrix}. \qquad (16)$$

The system of equations can be solved by inverting the A matrix and dividing the unknown variables by P, the surface pressure on the upper elastic layer,

$$\begin{Bmatrix} A'/P \\ B'/P \\ \cdot \\ \cdot \\ \cdot \\ \cdot \\ \cdot \\ \cdot \\ p'''/P \end{Bmatrix} = \begin{bmatrix} \\ \\ A \\ \\ \\ \end{bmatrix}^{-1} \cdot \begin{Bmatrix} -1 \\ 0 \\ 0 \\ -k_1/\rho\omega \\ 0 \\ \cdot \\ \cdot \\ \cdot \\ \cdot \end{Bmatrix}. \qquad (17)$$

The coefficients of A are given as

$$a_{1,2} = -\left[\lambda'\left(k_1^2 + \gamma'^2\right) + 2\mu'\gamma'^2\right] ,$$

$$a_{1,3} = 2i\mu' k_1 \gamma_s' ,$$

$$a_{2,1} = 2i\mu' k_1 \gamma' ,$$

$$a_{2,4} = \mu'\left(\gamma_s'^2 - k_1^2\right) ,$$

$$a_{2,9} = -1 ,$$

$$a_{3,1} = i\omega\gamma' ,$$

$$a_{3,4} = -\omega k_1 ,$$

$$a_{3,10} = -1 ,$$

$$a_{4,2} = -\omega k_1 ,$$

$$a_{4,3} = -i\omega\gamma_s' ,$$

$$a_{4,9} = 1/\rho(i\omega)^{1/2} ,$$

$$a_{5,1} = -\left[\lambda'\left(k_1^2 + \gamma'^1\right) + 2\mu'\gamma'^2\right]\sin \gamma' T_1 ,$$

$$a_{5,2} = -\left[\lambda'\left(k_1^2 + \gamma'^1\right) + 2\mu'\gamma'^2\right]\cos \gamma' T_1 ,$$

$$a_{5,3} = 2i\mu' k_1 \gamma_s' \cos \gamma_s' T_1 ,$$

$$a_{5,4} = -2i\mu' k_1 \gamma_s' \sin \gamma_s' T_1 ,$$

$$a_{5,5} = \left[\lambda''\left(k_1^2 + \gamma''^2\right) + 2\mu''\gamma''^2\right]\sin \gamma'' T_1 ,$$

$$a_{5,6} = \left[\lambda''\left(k_1^2 + \gamma''^2\right) + 2\mu''\gamma''^2\right]\cos \gamma'' T_1 ,$$

$$a_{5,7} = -2i\mu'' k_1 \gamma_s'' \cos \gamma_s'' T_1 ,$$

$$a_{5,8} = 2i\mu'' k_1 \gamma_s'' \sin \gamma_s'' T_1 ,$$

$$a_{6,1} = 2i\mu' k_1 \gamma' \cos \gamma' T_1 ,$$

$$a_{6,2} = -2i\mu' k_1 \gamma' \sin \gamma' T_1 ,$$

$$a_{6,3} = \mu'\left(\gamma_s' - k_1^2\right)\sin \gamma_s' T_1 ,$$

$$a_{6,4} = \mu'\left(\gamma_s' - k_1^2\right)\cos \gamma_s' T_1 ,$$

$$a_{6,5} = -2i\mu'' k_1 \gamma'' \cos \gamma'' T_1 ,$$

$$a_{6,6} = 2i\mu'' k_1 \gamma'' \sin \gamma'' T_1 ,$$

$$a_{6,7} = -\mu''\left(\gamma_s'' - k_1^2\right)\sin \gamma_s'' T_1 ,$$

$$a_{6,8} = -\mu''\left(\gamma_s'' - k_1^2\right)\cos \gamma_s'' T_1 ,$$

$$a_{7,1} = \gamma' \cos \gamma' T_1 ,$$

$$a_{7,2} = -\gamma' \sin \gamma' T_1 ,$$

$$a_{7,3} = ik_1 \sin \gamma_s' T_1 ,$$

$$a_{7,4} = ik_1 \cos \gamma_s' T_1 ,$$

$$a_{7,5} = -\gamma'' \cos \gamma'' T_1 ,$$

$$a_{7,6} = \gamma'' \sin \gamma'' T_1 ,$$

$$a_{7,7} = -ik_1 \sin \gamma_s'' T_1 ,$$

$$a_{7,8} = -ik_1 \cos \gamma_s'' T_1 ,$$

$$a_{8,1} = ik_1 \sin \gamma' T_1 ,$$

$$a_{8,2} = ik_1 \cos \gamma' T_1 ,$$

$$a_{8,3} = -\gamma_s' \cos \gamma_s' T_1 ,$$

$$a_{8,4} = \gamma_s' \sin \gamma_s' T_1 ,$$

$$a_{8,5} = -ik_1 \sin \gamma'' T_1 ,$$

$$a_{8,6} = -ik_1 \cos \gamma'' T_1 ,$$

$$a_{8,7} = \gamma_s'' \cos \gamma_s'' T_1 ,$$

$$a_{8,8} = -\gamma_s'' \sin \gamma_s'' T_1 ,$$

$$a_{9,5} = -\left[\lambda''\left(k_1^2 + \gamma''^2\right) + 2\mu''\gamma''^2\right] \sin \gamma'' T_2 ,$$

$$a_{9,6} = -\left[\lambda''\left(k_1^2 + \gamma''^2\right) + 2\mu''\gamma''^2\right] \cos \gamma'' T_2 ,$$

$$a_{9,7} = 2i\mu'' k_1 \gamma_s'' \cos \gamma_s'' T_2 ,$$

$$a_{9,8} = -2i\mu'' k_1 \gamma_s'' \sin \gamma_s'' T_2 ,$$

$$a_{9,12} = 1 ,$$

$$a_{10,5} = 2i\mu'' k_1 \gamma'' \cos \gamma'' T_2 ,$$

$$a_{10,6} = -2i\mu'' k_1 \gamma'' \sin \gamma'' T_2 ,$$

$$a_{10,7} = \mu'' \left(\gamma_s''^2 - k_1^2\right) \sin \gamma_s'' T_2 ,$$

$$a_{10,8} = \mu'' \left(\gamma_s''^2 - k_1^2\right) \cos \gamma_s'' T_2 ,$$

$$a_{10,11} = -1 ,$$

$$a_{11,5} = i\omega\gamma'' \cos \gamma'' T_2 ,$$

$$a_{11,6} = -i\omega\gamma'' \sin \gamma'' T_2 ,$$

$$a_{11,7} = -\omega k_1 \sin \gamma_s'' T_2 ,$$

$$a_{11,8} = -\omega k_1 \cos \gamma_s'' T_2 ,$$

$$a_{11,12} = -\gamma''' p''' / \rho''' \omega ,$$

$$a_{12,5} = -\omega k_1 \sin \gamma'' T_2 ,$$

$$a_{12,6} = \omega k_1 \cos \gamma'' T_2 ,$$

$$a_{12,7} = -i\omega\gamma_s'' \cos \gamma_s'' T_2 ,$$

$$a_{12,8} = i\omega\gamma_s'' \sin \gamma_s'' T_2 ,$$

$$a_{12,11} = 1/\rho''' \left(i\omega\nu'''\right)^{1/2} ,$$

and

$$a_{12,12} = k_1/\rho'''\omega .$$

All unlisted coefficients are zero. Since the impedance functions are desired to complete the pressure analogy, we obtain them from the matrix equations and express them in terms of the inverted matrix A,

$$\frac{v_2}{p} = Z = \left(a^{-1}_{10,1}\right)(-1) + \left(a^{-1}_{10,4}\right)\left(\frac{-k_1}{\rho\omega}\right)$$

and

$$\frac{\sigma_{12}}{p} = Y_1 = \left(a^{-1}_{9,1}\right)(-1) + \left(a^{-1}_{9,4}\right)\left(\frac{-k_1}{\rho\omega}\right) ,$$

where a^{-1}_{ij} indicates that particular entry in the inverse matrix A^{-1}.

Equation (11) for the pressure spectrum can now be evaluated by substituting the values of $Z(k,\omega)$ and $Y(k,\omega)$, as

$$\tilde{P}(k,\omega) = \frac{D_{ij}D^{+}_{k\ell}}{\left|\gamma + \rho\omega\left(a^{-1}_{10,1}\right) + k_1\left(a^{-1}_{10,4}\right) + k_1\left(a^{-1}_{9,1}\right) + \frac{k_1^2}{\rho\omega}\left(a^{-1}_{9,4}\right)\right|} \rho^2 U^3 h^5 Q_{ijk\ell} \quad . \tag{18}$$

PRESSURE SPECTRUM RESULTS

Since the manual inversion of a 12 by 12 complex matrix is a formidable task, the solution to equation (17) was performed by a double-precision complex matrix-inversion subroutine from the commercially-available international mathematical and statistical libraries (IMSL) on a VAX 11/780 computer. To check the accuracy of the solution algorithm, the two cases of a single steel plate of 1 or 5 cm backed by water at 10 kHz, given by Dowling, are compared with similar cases here. The pressure spectrum Dowling shows for those cases are given on the lower face of the elastic slab. To obtain a similar pressure spectrum, we must alter equation (18).

From equation (17), the ratio p'''/p is given by

$$\frac{p'''}{p} = -\left(a^{-1}_{12,1}\right) - \frac{k_1}{\rho\omega}\left(a^{-1}_{12,4}\right) \quad . \tag{19}$$

Substituting equation (19) into equation (18) gives the pressure spectrum on the lower surface,

$$\tilde{P}(k,\omega) = \frac{\left|D_{ij}D^{+}_{k\ell}\right|^2 \left|-\left(a^{-1}_{12,1}\right) - \frac{k_1}{\rho\omega}\left(a^{-1}_{12,4}\right)\right|^2}{\left|\gamma + \rho\omega\left(a^{-1}_{10,1}\right) + k_1\left(a^{-1}_{10,4}\right) + k_1\left(a^{-1}_{9,1}\right) + \frac{k_1^2}{\rho\omega}\left(a^{-1}_{9,4}\right)\right|^2} \rho^2 U^3 h^5 Q_{ijk\ell} \quad . \tag{20}$$

Figures 2 and 3 are plots of a nondimensional function, F, which shows the characteristics of the pressure spectrum on the lower surface. The function, F, is defined as

$$\tilde{F}(k,\omega) = \frac{\frac{\omega}{c}\left|-\left(a^{-1}_{12,1}\right) - \frac{k_1}{\rho\omega}\left(a^{-1}_{12,4}\right)\right|}{\left|\gamma + \rho\omega\left(a^{-1}_{10,1}\right) + k_1\left(a^{-1}_{10,4}\right) + k_1\left(a^{-1}_{9,1}\right) + \frac{k_1^2}{\rho\omega}\left(a^{-1}_{9,4}\right)\right|} \quad . \tag{21}$$

The plots show 20 log F versus nondimensional $K^{+} = kc/\omega$. These plots compare exactly with those in Dowling[3] of 1- and 5-cm bare steel plates backed by water at 5 and 10 kHz, respectively.

The major application of the wall-pressure analogy in this report will be to investigate the surface-pressure spectrum given by equation (18) for cases

where the upper fluid is water, the lower fluid is air, and the medium is a combination of viscoelastic and steel materials. The pressure spectrum is given both on the top surface of the upper layer and on the interface between the two elastic layers. As a base-case comparison for the material combinations to follow, we show the surface-pressure spectrum on the upper surface of a 1-in. steel plate at 5 and 10 kHz in figures 4 and 5. All pressure spectra plotted in this report are similar to those in figures 2 and 3 in that they are plots of the nondimensional function F evaluated at the appropriate surface. To plot the absolute pressure magnitudes, we would need to know the values of the $Q_{ijk\ell}$ function. Since very few measurements, if any, have been made of the turbulent-source cross-correlation terms, our intention here is to show relative reductions or increases in pressure spectrum and not absolute magnitude. Also, the structure of the low-wavenumber content of the pressure spectrum can be examined for local maxima and minima.

It is clear from figures 2 through 5 that the pressure spectrum always contains a discontinuity at $K^+ = 1$. At 5 and 10 kHz in figures 4 and 5, another discontinuity appears moving from right to left across the wavenumber spectrum as the frequency increases. For 5 kHz, the flexural wavelength of a 1-in. steel plate in vacuo corresponds to $K^+ = 1.36$. At 10 kHz, this value is close to $K^+ = 1$. One can see that the flexural wavelength of the plate introduces another singularity into the pressure spectrum. This singularity moves to lower wavenumbers with increasing frequency until it reaches $K^+ = 1$. At higher frequencies, the singularity does not appear to move below $K^+ = 1$. Elastic surfaces that have a flexural propagation speed greater than that of an acoustic wave in the fluid do not appear to have a double singularity in the pressure spectrum due to their flexural waves. This detailed behavior is consistent with general theoretical observations of Dowling.[2]

Now, we can proceed to investigate the relative dB gains or reductions in the turbulent wall pressure spectrum as a result of viscoelastic surfaces applied to the 1-in. thick bare plates. The viscoelastic properties we refer to are obtained by using a complex shear and Young's modulus with a specified thickness and mass density. Figures 6 and 7 show the top- and mid-surface pressure spectrum (mid surface is the interface between the two elastic media) for a 1-in. steel plate at 10 kHz covered with 3 in. of viscoelastic material having the properties $G = 43 + 4.3i$ psi, $E = 129.1 + 12.9i$ psi, and $\rho = 0.0001$ lb-s^2/in.^{4}. This material represents a fairly "compliant" surface with a density near that of water.

The singularity due to the flexural-plate speed is now seen to be reduced in magnitude in the top-surface spectrum at 10 kHz from that of the bare steel plate but remains quite distinct in the mid-surface spectrum. In the top-surface spectrum, the elastomer-coated plate demonstrates a noticeable reduction in the pressure spectrum for wavenumbers $0.5 < K^+ < 1$. There is a slightly larger reduction for $K^+ > 1.1$. This suggests that this candidate material may actually reduce the level of turbulent "noise." However, in figure 7, which shows the mid-surface pressure spectrum, the dramatic reduction from that on the bare plate corresponds, for the most part, to transmission loss through the layer. Also appearing in figure 7 is a singularity occurring at $K^+ \approx 0.3$. This singularity actually occurs in most of the plots and corresponds to the compressive-wave speed of the steel plate given by

$$C_c = \sqrt{\frac{E}{\rho(1 - \nu^2)}} . \qquad (22)$$

Except for this singularity, the supersonic regime of the top-surface pressure in the figure 6 spectrum appears to have a very flat profile. The rise in pressure level with movement from $0 < K^+ < 1$ for the bare steel plate does not occur in the case of this covered plate. This particular case indicates a reduction in the top-surface pressure-spectrum level for some supersonic wavenumber elements and for all the subsonic wavenumbers shown in this case.

Figures 8 and 9 show the same 3-in. viscoelastic coating at 5 kHz. Again, we see a reduction in the surface pressure at the top surface of the coating from that on the bare steel plate and a significant transmission loss is evident in the mid-surface pressure spectrum. The elastomer appears to have less of an effect on the pressure spectrum at lower frequencies in that the spectrum does not attenuate as dramatically (on the mid-surface at higher wavenumber) for 5 kHz as it did for 10 kHz. On the top surface, the flat level of the pressure spectrum is, again, seen to be in the supersonic regime. The examples in figures 6 through 9 show the frequency dependence of the pressure spectrum for a fixed set of material properties. It is more likely, though, that real material properties would also change with frequency.

Figures 10 and 11 show results for a 1-in. steel plate coated with an elastic material layer having the properties, at 5 kHz, $G = 90{,}000$ psi, $E = 252{,}000$ psi, and $\rho = 0.0001$ lb-s^2/in.^{4}. In figures 12 and 13, 5 percent damping has been added to the above shear and Young's moduli. The purpose of using this particular material is to demonstrate the effect on the pressure spectrum when a steel plate is coated with a material having its flexural, compressive, and shear speeds all in the vicinity of the acoustic-wave speed. When we try to find surfaces that reduce turbulent-noise levels, we see that a surface with propagation speeds near the wavenumber region of interest will introduce additional singularities in the pressure spectrum, as is demonstrated by this particular material.

One of the most noticeable features in figures 10 through 13 is the increase in the pressure spectrum at higher wavenumbers over that of the bare steel plate. This occurs for the damped, as well as the undamped, case. In addition, the flat level of the pressure spectrum on the top surface for supersonic wavenumbers, seen for the softer viscoelastic surface shown in figures 6 and 8, is no longer shown. Instead, the pressure reaches a local maximum around $K^+ \approx 0.75$. If one looks at the undamped top-surface spectrum versus the undamped mid-surface spectrum, figures 10 and 11, it is evident that the pressure spectrum is greater on the mid surface than on the top surface for $K^+ < 0.75$. However, with movement out to $K^+ > 2$, the pressure spectra at both surfaces are nearly equal in magnitude.

The effect of a small amount of damping in shear and Young's moduli is most dramatic in figure 13, the mid-surface pressure. The structure of the pressure spectrum for $1 < K^+ < 1.75$ has changed dramatically from the undamped case in figure 11. Nulls not seen before in the pressure spectrum are now

evident. The nulls probably also exist in the undamped case. However, the very narrow extent of these nulls is such that, for the undamped case, the finite points used to plot the curve are spaced too far apart to reveal the nulls. Damping serves to broaden the wavenumber extent of the nulls, giving enough span so that the nulls now appear.

In both the mid- and top-surface pressure spectra, damping in the coating appears to control the magnitudes of the singularities but does not change their location on the wavenumber axis. It would appear that very heavy damping might remove the singularities for $K^+ > 1$. The surface-pressure spectrum for the lightly damped coating of figure 12, when compared to that for the bare steel plate, shows a marked difference. However, it is difficult to assess visually whether the coating results in more or less turbulent noise because of the complexity of the wavenumber spectra. One final interesting feature is the fact that damping increases the level of the local maximum in the pressure spectrum at $K^+ \approx 0.75$ for both the top and mid surface. It is not certain why this is so.

CONCLUSIONS

The Dowling pressure analogy for an elastic medium under a turbulent-boundary-layer flow has been extended to a two-layered elastic medium. This analogy predicts the nature of the relative pressure spectrum at any surface in the elastic medium and can demonstrate graphically the results of different combinations of isotropic elastic and viscoelastic materials. The assumption applied in the analogy to the turbulent-source terms limits the range of applicability of the model to low wavenumbers relative to the convective peak. In addition, large surface motion would violate the assumption of a linear relationship between structural displacement and fluid velocity. For the low-wavenumber region, this model provides a unique way of looking at multilayered systems and their behavior relative to an unspecified turbulent-boundary-layer loading.

Specifically, we have shown the pressure spectra of two different viscoelastic materials on a steel plate. The first viscoelastic coating chosen showed local reductions in the pressure spectrum on the top surface and on the mid surface. The second viscoelastic coating was chosen to demonstrate that surfaces which have propagation speeds near the acoustic-wave speed can introduce new structure into the pressure wavenumber spectrum, similar to an observation by Dowling[2] on coatings with sound speeds less than that of the turbulent fluid.

It was also shown that plate flexural and compressional singularities can be affected by damping in the elastic layers. This model is intended to provide a means by which the performance of coatings applied to parent material can be investigated as to their influence on turbulent-boundary-layer noise levels. The inclusion of shear waves in the elastic layers and surface shears due to the turbulent flow make the model more complete for use in predicting wall pressure spectra.

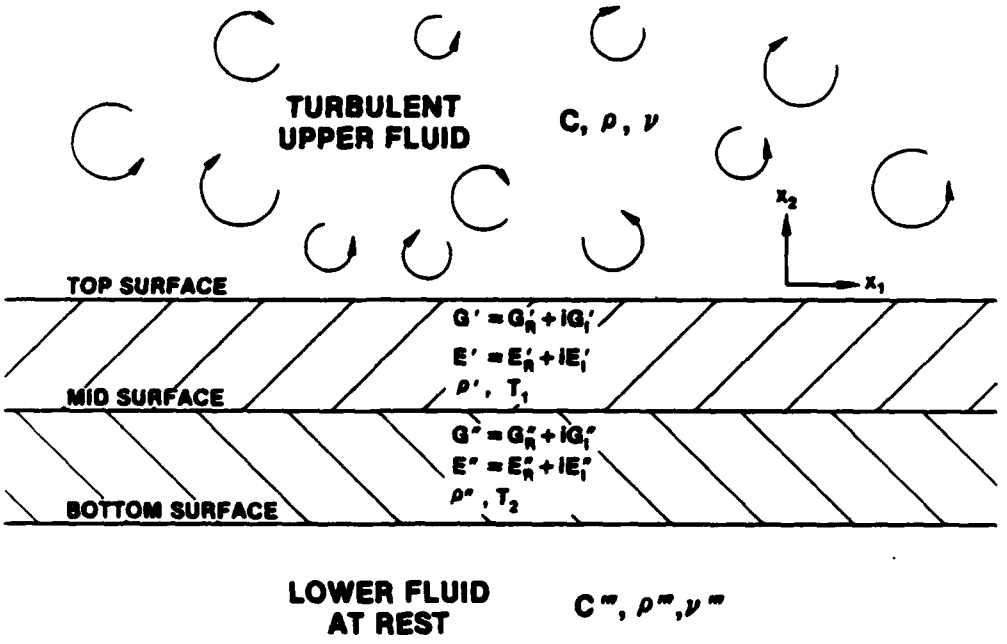

Figure 1. Geometry of the Two-Layered Medium and Flow Field

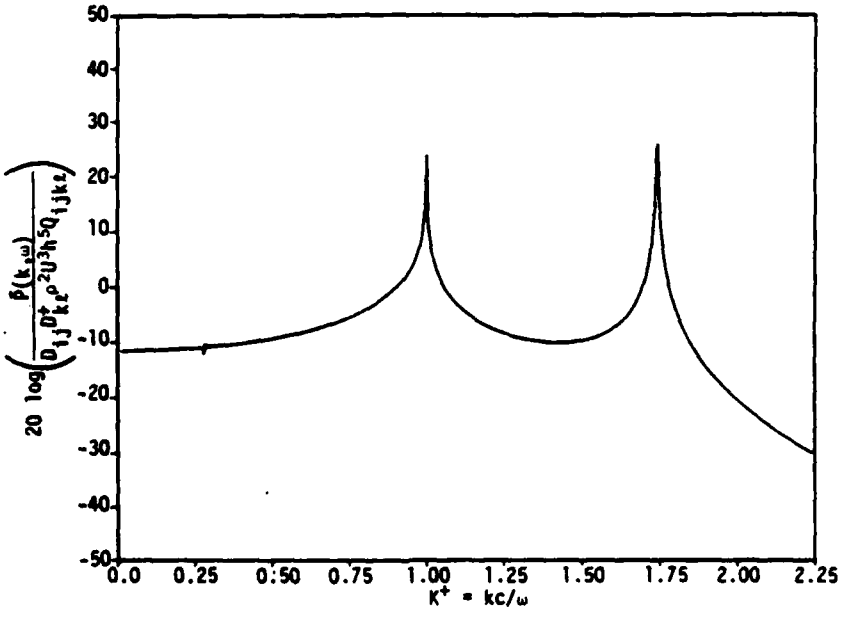

Figure 2. Lower Surface Pressure Spectrum on a Bare 0.4-in. Steel Plate at 10 kHz

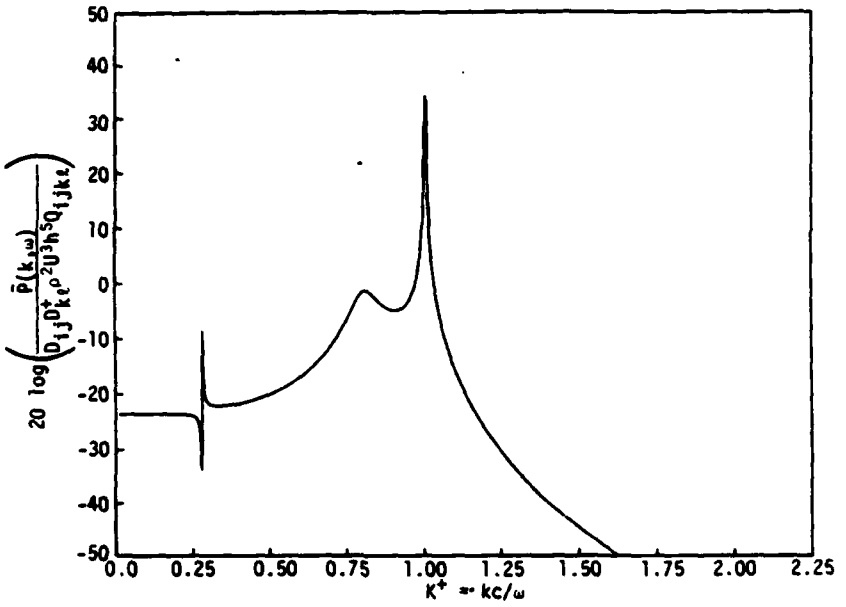

Figure 3. Lower Surface Pressure Spectrum on a Bare 1-in. Steel Plate at 10 kHz

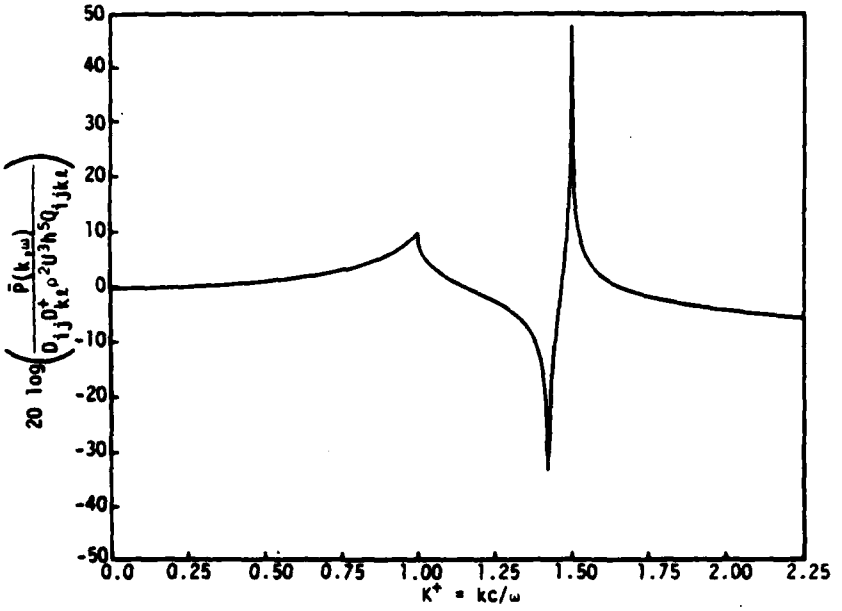

Figure 4. Upper Surface Pressure Spectrum on a Bare 1-in. Steel Plate at 5 kHz

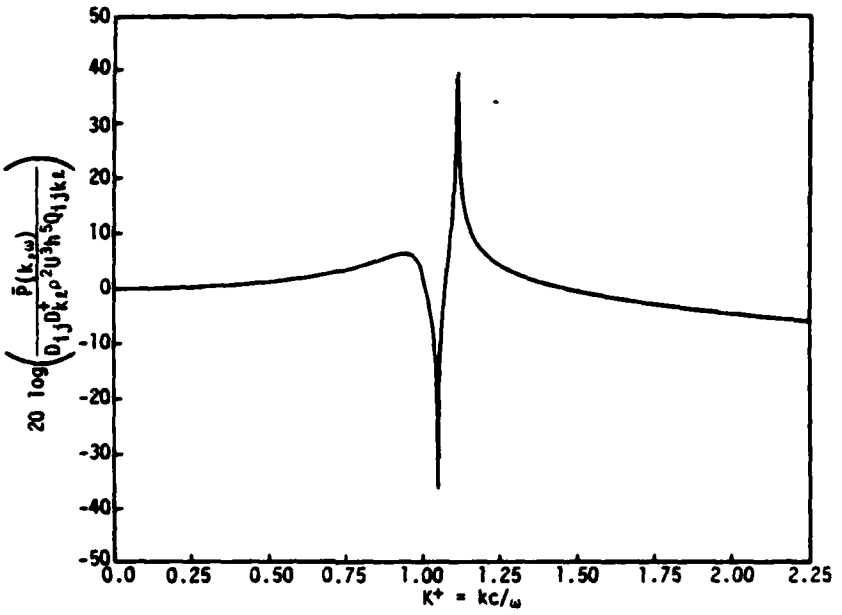

Figure 5. Upper Surface Pressure Spectrum on a Bare 1-in. Steel Plate at 10 kHz

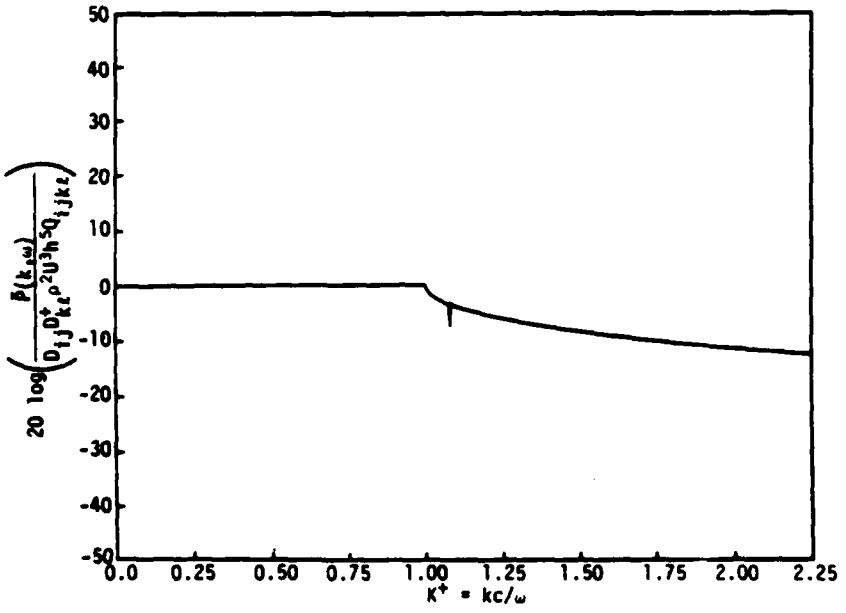

Figure 6. Upper Surface Pressure Spectrum for a 3-in. Viscoelastic Coating on a 1-in. Steel Plate at 10 kHz, Coating 1

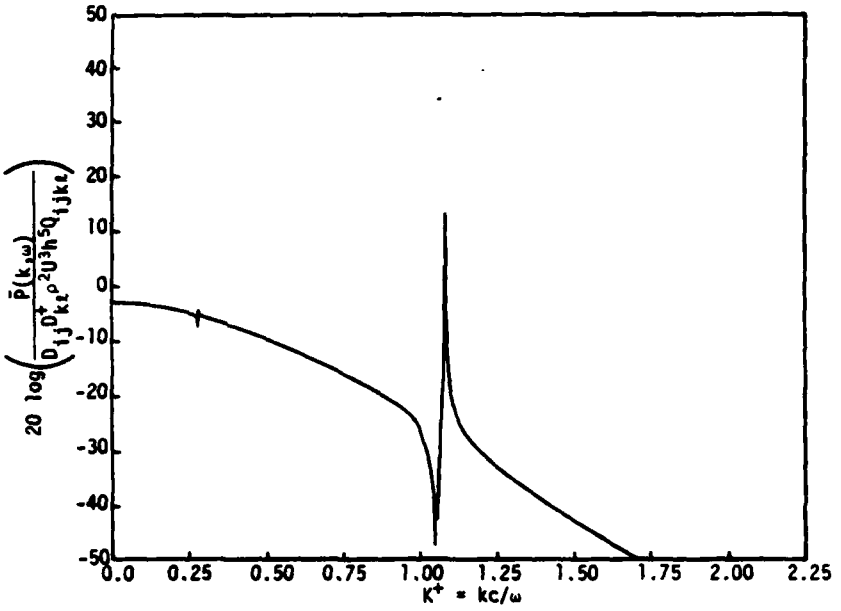

Figure 7. Middle Surface Pressure Spectrum for a 3-in. Viscoelastic Coating on a 1-in. Steel Plate at 10 kHz, Coating 1

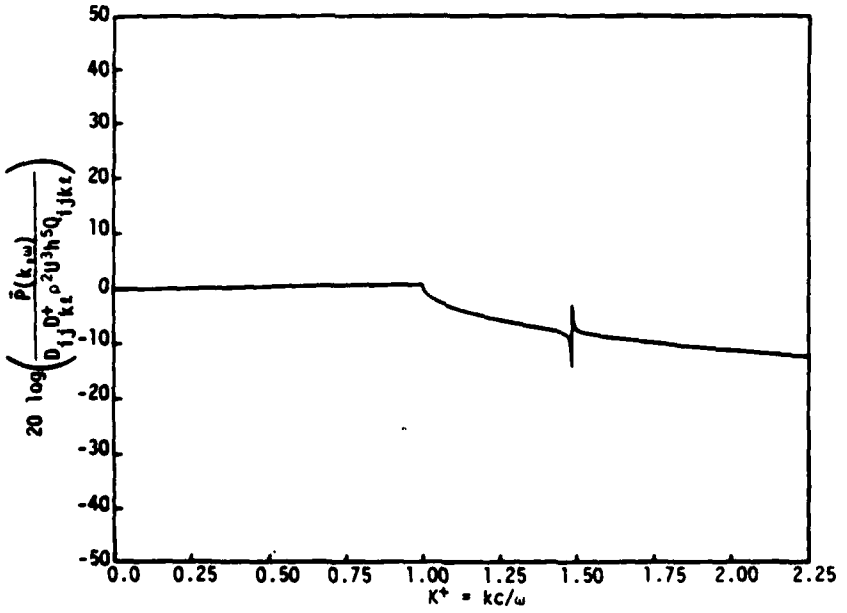

Figure 8. Upper Surface Pressure Spectrum for a 3-in. Viscoelastic Coating on a 1-in. Steel Plate at 5 kHz, Coating 1

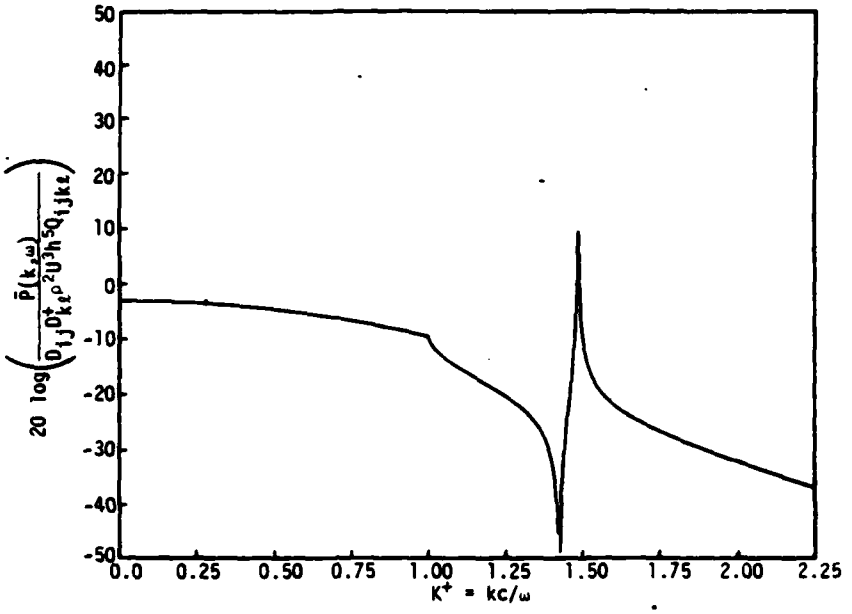

Figure 9. Middle Surface Pressure Spectrum for a 3-in. Viscoelastic Coating on a 1-in. Steel Plate at 5 kHz, Coating 1

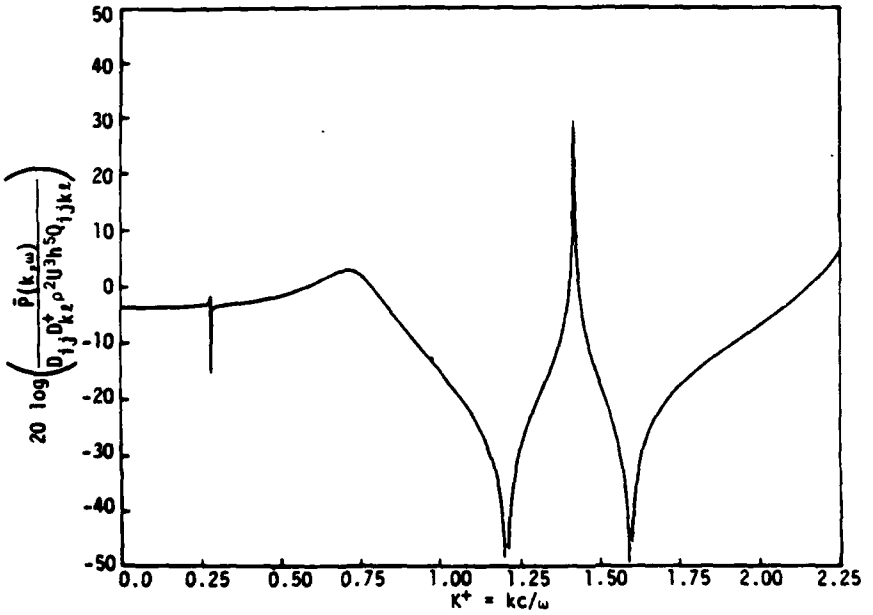

Figure 10. Upper Surface Pressure Spectrum for a 3-in. Elastic Coating on a 1-in. Steel Plate at 5 kHz, Coating 2

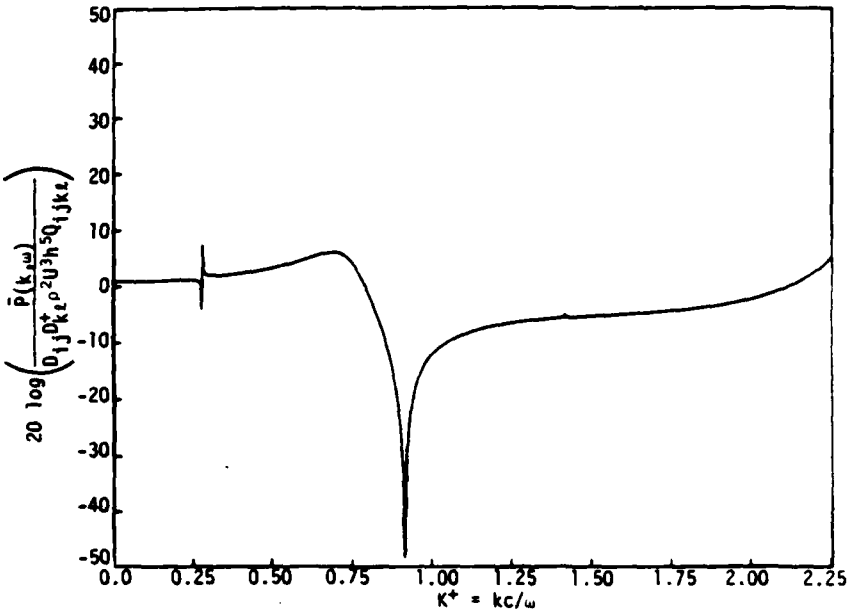

Figure 11. Middle Surface Pressure Spectrum for a 3-in. Elastic Coating on a 1-in. Steel Plate at 5 kHz, Coating 2

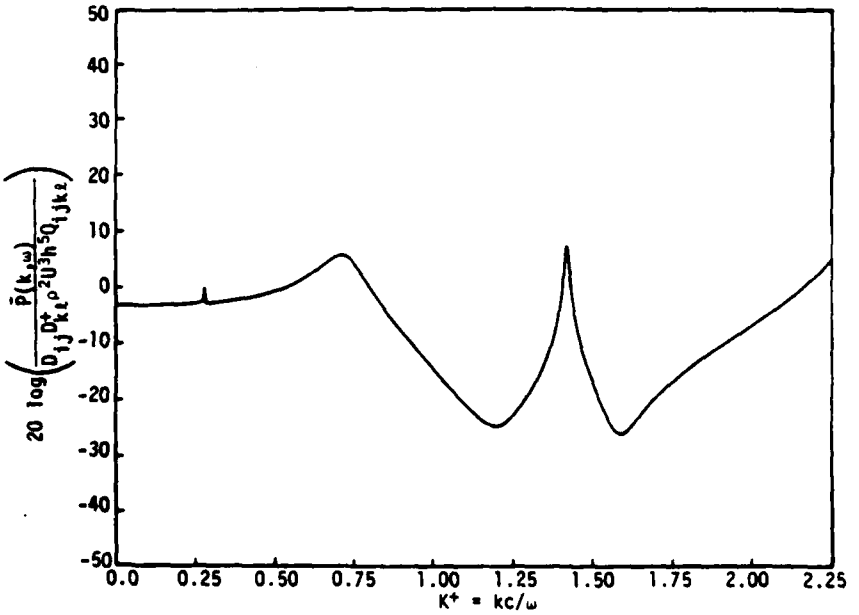

Figure 12. Upper Surface Pressure Spectrum for a 3-in. Viscoelastic Coating on a 1-in. Steel Plate at 5 kHz, Coating 3

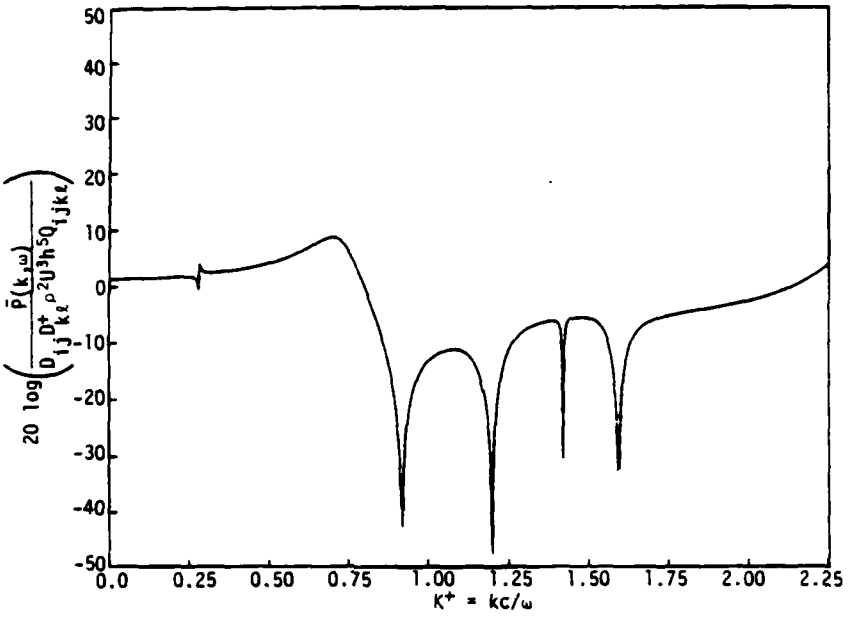

Figure 13. Middle Surface Pressure Spectrum for a 3-in. Viscoelastic Coating on a 1-in. Steel Plate at 5 kHz, Coating 3

REFERENCES

1. A. P. Dowling, "Flow-Acoustic Interaction Near a Flexible Wall," Journal of Fluid Mechanics, vol. 128, 1983, pp. 181-198.

2. A. P. Dowling, "The Low Wavenumber Wall Pressure Spectrum on a Flexible Surface," Journal of Sound and Vibration, vol. 88, 1983, pp. 11-25.

3. A. P. Dowling, "Sound Generation by Turbulence Near an Elastic Wall," Journal of Sound and Vibration, vol. 90, 1983, pp. 309-324.

4. L. M. Brekhovskikh, Waves in Layered Media, Academic Press, NY, 1960.

INITIAL DISTRIBUTION LIST

Addressee	No. of Copies
OUSDR&E (Research & Advanced Technology)	2
ONR, ONR-220, -410, -425AC, -430	4
CNM, MAT-051	1
NRL, Code 5844 (Dr. J. R. Hansen), 5130 (Dr. R. T. Menton)	3
NAVSEASYSCOM, SEA-55x4	1
NAVAIRDEVCEN	1
NOSC, Code 8302, 6565 (Library)	2
NAVSWC	1
DWTNSRDC BETH, Code U31 (Dr. W. Blake, Dr. G. Maidanik)	2
NAVPGSCOL	1
DTIC	2
BBN (Dr. N. Martin) Contract No. N00140-83-GBA10-005	1
CHASE, INC., Cambridge, MA (Dr. D. Chase) Contract No. N00140-84-DJA40-001	1

END

FILMED

10-85

DTIC